

1 **Deployment of a *Vibrio cholerae* ordered transposon mutant library in a quorum-
2 competent genetic background**

3 Nkrumah A. Grant^{1,2,3*}, Jordan T. Sontz,⁴ Christopher M. Waters^{2,3,4*}

4

5 ¹Department of Microbiology, University of Illinois Urbana-Champaign, Urbana, IL

6 ²Department of Microbiology and Molecular Genetics, Michigan State University, East Lansing,
7 MI

8 ³BEACON Center for the Study of Evolution in Action, Michigan State University, East
9 Lansing, MI

10 ⁴MSU College of Osteopathic Medicine, Michigan State University, East Lansing, MI

11

12 *Correspondence to: grantnkr@illinois.edu or watersc3@msu.edu

13

14 **Abstract**

15 Cholera is a severe diarrheal disease that claims approximately 30,500 lives annually, mainly in
16 regions with limited access to clean water. *Vibrio cholerae*, the causative agent, has sparked
17 seven pandemics in recent centuries, with the current one being the most prolonged. *V. cholerae*
18 pathogenesis hinges on its ability to switch between low and high cell density gene regulatory
19 states, enabling transmission between host and the environment.

20 Previous researchers created a transposon mutant library for *V. cholerae* to support investigations
21 aimed toward uncovering the genetic determinants of its pathogenesis. However, subsequent
22 sequencing uncovered a mutation in the gene *luxO* of the parent strain, rendering mutants unable
23 to exhibit high cell density behaviors. In this study, we used chitin-independent natural
24 transformation to move transposon insertions from these low cell density mutants into a wildtype
25 genomic background. Library transfer was aided by a novel gDNA extraction we developed
26 using thymol, which also showed marked vibrio-specific activity. The resulting Grant Library
27 comprises 3,102 unique transposon mutants, covering 79.8% of *V. cholerae*'s open reading
28 frames. Whole genome sequencing of randomly selected mutants demonstrates 100% precision
29 in transposon transfer to cognate genomic positions of the recipient strain. Notably, *luxO*
30 mutations transferred at a low frequency only with insertions near *luxO*. Our research uncovered
31 density-dependent epistasis in motility genes, relevant to *V. cholerae* pathogenesis. Additionally,
32 Grant Library mutants retain a plasmid conferring natural competence, enabling rapid, scarless
33 genomic editing. In summary, the Grant Library reintroduces organismal relevant genetic
34 contexts absent in the low cell density locked library equivalent.

35

36 **Introduction**

37 *Vibrio cholerae* is a human pathogen and the causative agent of the acute diarrheal disease
38 cholera. While cholera is a global threat, the disease is endemic in developing countries, where it
39 is estimated that there are between 1.3 to 4.0 million *V. cholerae* annual infections, resulting in
40 21,000 – 143,000 deaths (1, 2). Implementation of disease intervention strategies, including
41 increasing access to clean drinking water, provision of adequate healthcare infrastructure, and
42 educating citizens in communities at risk of disease spread, remains a top priority in the fight
43 toward eradicating cholera. As such, the Global Task Force on Cholera Control was founded in
44 2017 to support efforts aimed at reducing cholera burden by 90% before the year 2030 (3, 4).

45

46 To date there have been seven cholera pandemics. The seventh pandemic began in 1961
47 and is ongoing, marking it as the longest running cholera pandemic (5). *V. cholerae* strains are
48 grouped by surface antigens, including O polysaccharide, such that there are >200 serogroups
49 (6). Of these serogroups, only two, O1 and O139, host pandemic *V. cholerae* strains (7, 8).
50 Furthermore, pandemic strains from the O1 serogroup are further stratified into two biotypes
51 with the fifth and sixth pandemics caused by the Classical and the seventh caused by El Tor (9).

52

53 Like most vibrios, *V. cholerae* predominantly possesses two chromosomes (10, 11).
54 Whole genome sequencing of strains before and after the emergence of seventh pandemic *V.*
55 *cholerae* strains has proved to be an invaluable resource toward understanding its origin and
56 evolution. These analyses show *V. cholerae* El Tor originated from a nonpathogenic strain (12),
57 becoming a pathogen after acquiring two genomic islands (VSP-I and VSP-II), a prophage that
58 expresses cholera toxin (CTXφ), and 12 additional mutations that enhanced its transmissibility
59 (9, 13, 14). Recent work has also shown that these genomic changes contribute to seventh
60 pandemic *V. cholerae*'s long-term persistence in the estuarine environments they occupy (15).

61

62 Key to El Tor's transition to a pathogen is that it is naturally competent, granting it the
63 ability to take up DNA from the environment which can be integrated into the genome by
64 homologous recombination (16). Natural competence is a highly regulated process, and four
65 environmental factors are key determinants for driving this process. These include nutrient
66 limitation, extracellular signaling molecules, high cell density, and the presence of chitin (17–
67 19), which together coordinate the expression of the four regulators (HapR, TfoX, CRP, and
68 CytR) governing competence (20–23). Recent work has shown that expressing the master
69 regulator TfoX can circumvent the chitin requirement for natural competence in *V. cholerae* (19,
70 24). This discovery has allowed exploitation of chitin-independent natural competence as a

71 genetic tool for editing *Vibrio spp.* genomes (25–27), facilitating our understanding of the
72 functional relationships between genes and furthering our understanding of how *V. cholerae*
73 interfaces with its environment.

74

75 Our understanding of *V cholerae*'s ecology and evolution has also benefited from
76 transposon mutagenesis. In contrast to conventionally laborious genetic engineering approaches
77 for disrupting single genes to study their phenotypic effects, transposon mutagenesis allows the
78 simultaneous construction and screening of tens of thousands of mutants. Researchers have taken
79 advantage of transposon mutagenesis to construct nonredundant (ordered) mutant libraries,
80 where each nonessential gene has been inactivated and the individual mutants are arrayed across
81 the wells of 96-well microtiter plates (28–31). An ordered mutant *V. cholerae* library was
82 constructed in 2008 (32). The ordered library consists of >3,100 mutants, each with a Tn5-based
83 transposon insertion that confers kanamycin resistance. The mutant library has provided a public
84 resource enhancing *V. cholerae* genotypic and phenotypic investigations, supporting identifying
85 novel therapeutic targets for vaccine development (33), and increasing our understanding of the
86 *V. cholerae* virulome (34, 35), amongst other discoveries (36, 37).

87

88 Although significant research advances have been made in our understanding of *V.*
89 *cholerae* using mutants from this ordered mutant transposon library, the library was constructed
90 in a laboratory acquired quorum sensing mutant of *V. cholerae*. Quorum sensing, the process of
91 cell-to-cell communication in bacteria, allows cells to undergo global changes in gene expression
92 as the bacteria transition from low to high cell density. This transition can influence behaviors
93 like host immunity escape (38), virulence factor production (39–41), biofilm formation (42),
94 infectivity and environmental dissemination (43), and protection against phage predation (44).
95 This transition is mediated by extracellular autoinducers (45, 46) which impact the activity of
96 cytoplasmic regulators, including LuxO and HapR .

97

98 In the low-cell-density state, LuxO is phosphorylated leading to inhibition of *hapR*
99 mRNA translation via regulatory sRNAs, whereas at high-cell-density, LuxO is
100 dephosphorylated and inactive, resulting in HapR protein translation and the switch to high-cell-
101 density (41, 47). Recently, a presumably laboratory acquired mutation in *luxO*, *luxOG319S* was
102 discovered in some laboratory isolates of the widely used *V. cholerae* strain C6706 that locked
103 this strain in the low-cell-density state (48). After sequence validating mutants from the 2008
104 library, we observed the *luxOG319S* mutation, indicating it was present in the parent strain from
105 which the library was constructed. Thus, the 2008 ordered mutant library (32) is only partially

106 representative of how *V. cholerae* senses and responds to its environment and a new library in a
107 quorum sensing competent strain would greatly enhance our understanding of *V. cholerae*
108 ecology and evolution.

109

110 To overcome this limitation of the 2008 library, we use chitin-independent natural
111 competence to regenerate the defective ordered *V. cholerae* library in a quorum competent
112 C6706 genomic background. To streamline the transfer process, we developed a cost effective
113 gDNA extraction method using thymol (49). Compared to other methods, our approach is both
114 economical (\$0.64 per reaction vs \$2.85 per reaction) and efficient, enabling up to 200 gDNA
115 extractions in as little as 2.5 hours, in contrast to 25 reactions requiring >6 hours using
116 conventional methods. Using our methods, we successfully regenerated the library with a 99%
117 success rate, as indicated by growth on antibiotic selection growth media. Sequence validation of
118 randomly selected mutants from the regenerated library show that the transposon insertions
119 recombine into our recipient strain with 100% precision. Transfer of the *luxOG319S* mutation
120 was minimal and only occurred in genes located close to the transposon insertion site. Of
121 significance, we provide evidence for density-dependent epistasis in several genes within class
122 III of the flagellum biosynthesis gene clusters, an observation that undoubtedly extends to other
123 phenotypes, illustrating the utility of this new library. Lastly, we show that strains from the
124 library generated in this work – hereafter the Grant Library – can undergo additional edits using
125 chitin-independent natural competence. Taken together, the Grant Library represents an added
126 contribution in our efforts toward understanding *V. cholerae* behaviors under transcriptional
127 regulatory states that are representative of how this pathogen evolves and interfaces with its
128 environment.

129

130 **Materials and Methods**

131

132 **Bacterial matings**

133 To generate the library recipient strain used in this study, NG001, we mated wildtype *V. cholerae*
134 C6706 with an *E. coli* S17-λpir donor strain harboring plasmid pMMB-*tfoX-qstR* (generously
135 provided by Ankur Dalia, Indiana University). In short, we mixed equal volumes of donor and
136 recipient strains in the center of a Luria-Bertani agar plate which we incubated at 37°C for three
137 hours. Afterwards, we added 1 mL of LB media containing chloramphenicol (10 µg/mL, for
138 selection of plasmid in recipient strain) and polymyxin B (55.5 µg/mL, for counterselection of
139 the donor *E. coli* strain) to the plate, washed, and collected the mating spot into a borosilicate
140 glass culture tube, which we incubated overnight at 37°C with orbital shaking at 210 RPM.

141 **Media and buffers**

142

143 *Thymol cell lysis agent*

144 We prepared thymol at a stock concentration of 350 mM by dissolving thymol crystals in
145 dimethyl sulfoxide (DMSO). Thymol stocks were made in 15 mL which we stored at room
146 temperature on the lab bench until they were exhausted. We observed no differences in the lytic
147 activity of thymol during storage.

148

149 *gDNA extraction buffer*

150 We prepared solutions of a gDNA extraction buffer in two 500 mL volume parts. We prepared
151 solution one by mixing 80 mL of 1M Tris (pH 8.0), 56 mL of 0.5M EDTA (pH 8.0), 46.7 g
152 NaCl, and 3 g sodium metabisulfite, which we stirred until dissolved. We then adjusted this
153 solution to the final volume with dH₂O and autoclaved for 25 minutes. We prepared solution
154 two, sodium acetate (2.5M, pH 5.2), by dissolving 102.5 g of the salt in dH₂O, which we
155 sterilized using filtration. Prior to each extraction, we prepared a master mixture of solution one
156 and solution two by mixing 21 mL and 31.5 mL for every 100 samples processed, respectively.

157

158 **Strain revival**

159 We revived strains from the nonredundant library ((32); henceforth referred to as donor library)
160 in microplate format to maintain parity between it and that produced in this work. The donor
161 library was generously provided by the laboratories of Vic DiRita (plates: 2, 4-6, 8-10, 12-17,
162 19-33), Michigan State University, and Bonnie Bassler (plates: 1, 3, 7, 11, 18, 34), Princeton
163 University. Briefly, microtiter plates from the donor library were slightly thawed and 10 µl from
164 each well was inoculated into a deep-well microplate containing 550 µl of selective media
165 (Luria-Bertani broth + Kanamycin (100 µg/ml) in each of the 96 wells. We revived the recipient
166 library strain, NG001, in a 250 ml baffled flask containing 25 ml of selective media (Luria-
167 Bertani broth + chloramphenicol (10 µg/ml)) to maintain plasmid *pmmB-tfoX-qstR* and 100
168 µg/ml isopropyl β-D-1-thiogalactopyranoside (IPTG) to induce natural competence. Unless
169 noted otherwise, we grew all cultures overnight (18 – 24h) at 37°C with orbital shaking at 210
170 RPM.

171

172 **Whole gDNA preparation**

173 The non-redundant donor library is comprised of 34 96-well plates of *Vibrio cholerae* mutants.
174 To extract genomic DNA from the donor library in a cost efficient and high-throughput fashion,
175 we developed an extraction method using a modified recipe of the gDNA extraction buffer

176 developed by Mantel and Sweigart, 2019 (accessed September, 2022, at
177 <https://www.protocols.io/view/quick-amp-dirty-dna-extraction-4r3l287zqlly/v1>). In brief, we
178 pelleted cells from overnight cultures of the donor library by centrifuging the deep-well plates at
179 4°C for 20 minutes. We then removed ~500 µl of supernatant from each well, resuspended the
180 cell pellet in 10 µl thymol (~35 mM final concentration), and incubated the plates at 64°C for 15
181 minutes. Thereafter, we added 500 µl of gDNA buffer to each well and incubated the plates at
182 64°C for an additional 45 minutes.

183

184 To clear culture supernatants of cellular debris, we transferred cell lysates from each well
185 into an E-Z 96™ Lysate Clearance Plate (<https://www.omegabiotek.com/product/e-z-96-lysate-clearance-plate/>). We then used a vacuum manifold to filter the supernatant through the plate,
186 which we collected in a second deep-well plate containing 200 µl of 100% cold isopropanol per
187 well. We then incubated the plates for 15 minutes at room temperature to precipitate genomic
188 DNA. Afterwards, we again used a vacuum manifold to filter the cell lysate containing our
189 gDNA through an E-Z 96™ DNA plate (<https://www.omegabiotek.com/product/e-z-96-dna-plates/?cn-reloaded=1>). According to the manufacturer, “E-Z 96™ plates are silica glass fiber
190 plates that can bind up to 50 µg of genomic DNA or 20 µg of plasmid DNA per prep.” After this
191 initial filtration, we washed our bound DNA, in sequence, using 500 µl of 70% and 95% ice cold
192 ethanol. We then added 100 µl of 1x TE buffer to each well and eluted genomic DNA from the
193 DNA plates into PCR plates by centrifugation (max speed, one minute).

194

195 **Chitin-independent natural competence for gDNA transfer**

196 After 18-24 h of overnight growth, we diluted the library recipient strain (NG001) 1:4 in 0.5x
197 instant ocean to which we added chloramphenicol (5 µg/ml) and IPTG (100 µg/ml). We then
198 added 200 µl of these competent cells to each well of a deep-well 96-well plate and added the
199 gDNA extracted from the donor library to a matched recipient well (final dilution 1:3). We then
200 incubated the deep-well plates overnight in a standing incubator at 30°C. Following the
201 overnight incubation, we added 400 µl of selective media (Luria-Bertani broth +
202 chloramphenicol (5 µg/mL) + kanamycin (100 µg/mL)) to each well and incubated the plates at
203 37°C in a standing incubator for 48 h (Fig. 1). We determined transformation success by spot
204 plating 3 µl of each well onto selective LB agar plates (Luria-Bertani agar + chloramphenicol (5
205 µg/mL) + kanamycin (100 µg/mL)), which we grew overnight at 37°C (Fig. S1).

206

207 **Grant Library transformation efficiency analysis**

210 We created a comprehensive plate indices file (Dataset S1) covering all possible wells within the
211 donor library (P1A1 to P34D6; 3,210 wells). Using this file, we developed a script to compare it
212 with a modified version of supplementary dataset 3 from Cameron et al., 2008 (Dataset S2),
213 which allowed us to identify empty wells (86) and those containing mutants (3,124). Our
214 comparative analysis also flagged duplicate entries in supplementary dataset 3 of the donor
215 library (Dataset S3).

216

217 While constructing the Grant Library, we meticulously documented the outcomes of
218 growth on selective media following chitin-independent natural transformation of the donor
219 library: True Positives (3,102 wells), False Negatives (22 wells expected to grow but didn't),
220 True Negatives (71 blank wells that didn't transfer), and False Positives (15 blank wells that
221 transferred unexpectedly). These values served as inputs for a binary confusion matrix (50),
222 providing a comprehensive assessment.

223

224 **TnFGL3 transposon insertion site identification**

225

226 *Genome Sequencing*

227 We randomly selected 23 mutants from the Grant library to identify the transposon insertion site.
228 Strains were incubated overnight in 3 ml of LB + Kanamycin (100 µg/ml) and DNA was
229 extracted from 1 ml of culture using a Wizard ® Genomic DNA Purification Kit following the
230 manufacturer's instructions. DNA was rehydrated overnight at 4°C in 50 µl of TE buffer. Library
231 preparation was performed by SeqCoast Genomics using an Illumina DNA Prep tagmentation kit
232 and unique dual indexes. Samples were multiplexed and sequenced on the Illumina NextSeq2000
233 platform using a 300-cycle flow cell kit to produce 2x150 bp paired reads. Read demultiplexing,
234 read trimming, and run analytics were performed using DRAGEN v3.10.11, an on-board analysis
235 software on the NextSeq2000. Raw sequencing data generated during this study are available in
236 the following public Github repository (<https://github.com/NkrumahG/Grant-Library-Construction>)

237

239 *Reference genomes*

240 The reference genomes for *V. cholerae* strains used in this study were downloaded from NCBI
241 GenBank. The chromosome accession numbers for chromosomes I and II are, NZ_CP028827.1
242 (2,975,504 bp) and NZ_CP028828.1 (1,072,331 bp) for strain N16961, and NZ_CP046844
243 (3,019,938 bp) and NZ_CP046845 (1,070,359 bp) for strain C6706, respectively. The sequence
244 map for plasmid pSC189 was downloaded from addgene

245 (<https://www.addgene.org/browse/sequence/36279/>), and the sequence for pMMB-*tfoX-qstR* was
246 provided by Ankur Dalia (Indiana University).

247

248 *Mutation calling*

249 We used consensus mode in *breseq* ((51), version 0.37) to align the paired-end reads for each of
250 the sequenced mutants to the reference genomes. The computational resources used to perform
251 *breseq* were provided by the Institute of Cyber-Enabled Research at Michigan State University.

252

253 *Ortholog identification*

254 We used Mauve ((52), snapshot _2015-02-25) to identify orthologs in whole genome sequences
255 of C6706 and N16961. Each pair of chromosomes were aligned using the progressive Mauve
256 method with default settings. In the Supplemental Information, we have included lists of all
257 orthologous gene pairs in *V. cholerae* N16961 and C6706 (Dataset S4) and the identity of genes
258 unique to N16961 (Dataset S5) and C6706 (Dataset S6). Additionally, we used Geneious to
259 extract, align, and visually display (Supplementary Information, Fig. S2 and S3) orthologous
260 gene pairs for the transposon mutants sequenced in this study.

261

262 **LuxO gain of function mutation identification**

263 Using supplementary dataset 3 provided for the donor library (32), we identified all potential
264 transposon mutants located within a 50 kb range, both upstream and downstream of *luxO*.
265 Subsequently, we developed a script that randomly picked 10 mutants from each side of *luxO*,
266 using 5 kb windows. Following this selection, we cultured these mutants in selective media (LB
267 + Kanamycin, 100 µg/mL) for 24 hours under standard conditions.

268

269 After the incubation, we extracted gDNA using the Wizard Genomic DNA Purification
270 Kit, following the manufacturer's instructions. The extracted genomic DNA was then diluted 1:2,
271 which we used as template for PCR amplification of the *luxO* gene. The *luxO* gene was
272 amplified with Q5 polymerase using the following primers: forward primer 5`-
273 GGCTATGCAACATAATCAAATCTTG-3` and reverse primer 5`-
274 GCTTGTTGATCCATTCTCTCAT-3`. PCR conditions included an initial denaturation at
275 98°C for 2 minutes, followed by 29 cycles of denaturing at 98°C for 30 seconds, annealing at
276 63°C for 30 seconds, and extension at 72°C for 1 minute. A final extension step was
277 performed at 72°C for 5 minutes.

278

279 Following the PCR amplification, we validated amplification of *luxO* using gel
280 electrophoresis. We then used the Wizard SV Gel and PCR Clean-Up System to purify our *luxO*
281 PCR product. Sanger sequencing of the purified *luxO* allele was performed using the reverse
282 primer 5`-TGCGATAGATGGTTGACGGG-3` by the Research Technology Support Facility
283 (RTSF) at Michigan State University. We imported the Sanger Sequence read data into Geneious
284 (53) and aligned it to *luxO* (*V. cholerae* chromosome I, C6706), allowing comprehensive
285 analysis and visualization of our sequenced mutants, with special attention to amino acid position
286 319, the site of the *luxO* gain of function mutation *luxOG319S* (48).

287

288 **Motility Assay**

289 We screened mutants with presumptive TnFLG3 transposon insertions in known motility genes.
290 Strains were grown in a deep-welled 96-well plate overnight at 37°C in selective media (LB +
291 Kanamycin) and on the following day, we used toothpicks to manually stab each strain into
292 motility plates containing LB and 0.35% agar. Plates were incubated at 37°C for 24 h, and the
293 motility zones were recorded with a gel imager. The area of the motility zones was measured
294 computationally using the Hough Circle Transform package from the UCB vision plugin in Fiji
295 (54).

296

297 **Data accessibility**

298 All of the data generated including Datasets S1-S6, and analysis scripts used in this work are
299 available in the GitHub repository at <https://github.com/NkrumahG/Grant-Library-Construction>.

300

301

302 **Results and Discussion**

303

304 **Chitin-independent transfer of transposons from donor library strains into a quorum-
305 competent *V. cholerae* genetic background is remarkably efficient.** We hypothesized that the
306 transposon insertions within the genomes of the quorum-incompetent *V. cholerae* strain
307 generated in Cameron et. al., 2008 could be transferred to a quorum-competent wildtype *V.*
308 *cholerae* strain using natural competence. To test this, we extracted gDNA from each mutant in
309 donor library using an in-house method involving thymol lysis and alcohol precipitation.
310 Subsequently, we co-incubated this gDNA with a wildtype *V. cholerae* strain (C6706) carrying a
311 plasmid that expresses the natural competence master regulator, TfoX, upon induction with IPTG
312 (Materials and Methods).

313

314 The donor library consists of 34 plates arrayed from P1A1 to P34D6, for a total 3,210
315 possible wells containing transposon mutants. Upon examination of supplementary data table 3
316 for the donor library, we discovered that 86 wells were not listed, and some of the mutants were
317 recorded multiple times. With these considerations, we expected growth for 3,124 unique
318 transposon mutants after conducting our natural transformation protocol.

319

320 To verify the presence of transposon insertions in the Grant library mutants, we spot-
321 plated each mutant on LB medium supplemented with kanamycin. Of the 3,124 unique
322 transposon mutants we expected to grow on the plates, 3,102 mutants (99.2%) exhibited growth
323 (Fig. S1). None of the 22 missing mutants, which were expected to grow, showed growth in
324 selective media during overnight revival of donor library freezer stock. This suggests that these
325 mutants might no longer viable perhaps due to low culture density upon freezing or death
326 resulting from repeated freeze-thaw cycling during long-term storage of the donor library. In the
327 cases where we anticipated no growth, 71/86 (82.0%) did not grow on selective media.

328

329 To evaluate the performance of our library transfer approach, we utilized a confusion
330 matrix (Fig. 2). The results of this analysis indicate that our approach was highly accurate and
331 precise, with a high recall (F1 score = 0.9941) and a low False Discovery Rate (0.0070). These
332 results unequivocally demonstrate the remarkable efficiency of using chitin-independent natural
333 competence to transfer the transposons into a quorum-competent strain. The transference process
334 was made possible through our in-house gDNA extraction method, involving thymol cell lysis
335 and alcohol precipitation, affirming the suitability of this gDNA preparation for downstream
336 applications. Indeed, this suitability was confirmed when we employed thymol-extracted DNA
337 as a template in PCR, with no observed inhibitions.

338

339 **Transposons from the donor library homologously recombine into the recipient genome**
340 **with 100% precision.** The frequency of genome edits by homologous recombination in *Vibrio*
341 *spp.* is highest when there are at least 2 kb arms of homology flanking the genomic sequence
342 being altered (25). Given this requirement, the observation that the recipient strains grew after
343 incubation on selective media (Fig. S1) was suggestive that transposons correctly integrated into
344 the homologous site of the recipient's genome. To validate our supposition, we randomly
345 selected 23 mutants, isolated gDNA, and sequenced whole genomes. Subsequently, we aligned
346 the sequenced reads to four reference sequences using breseq (51). The reference sequences
347 included *V. cholerae* chromosomes I and II, and the plasmid conferring natural competence. A
348 fourth reference sequence (pSC189) containing sequences associated with the transposon was

349 also included as a “genomic lure” to capture reads that mapped to the transposon. When
350 examining the breseq output, we specifically looked for instances where new junctions were
351 created between chromosomes I or II (depending on which chromosome the gene targeted for
352 homologous recombination was located) and pSC189. Such a junction would indicate a
353 transposon integration event. Fig. 3 is an example breseq output from one such alignment, which
354 reports the transposon insertion site in chromosome II, including the basepair position it is
355 located.

356

357 The parent strain of both the donor and recipient libraries is *V. cholerae* El Tor C6706.
358 However, when the donor library was generated in 2008, transposon insertion sites were mapped
359 to reference genomes of *V. cholerae* El Tor strain N16961 because it was the only *V. cholerae*
360 that had been sequenced for *Vibrio* spp. at that time (55). In this work, we mapped transposon
361 insertion sites to reference genomes of strain C6706. To identify whether transposons insertions
362 were in the correct site of our recipient strains, we performed whole genomic comparative
363 analysis of *V. cholerae* N16961 and C6706. When we performed this analysis, we found
364 chromosomes I and II differ in size between strains and are not syntenic (Fig. 4). Out of the
365 2,649 genes annotated in our reference genomes for chromosome I, 2,558 (96.6%) of genes are
366 shared between N16961 and C6706. Additionally, 21 genes (0.79%) are unique to N16961 and
367 70 (2.64%) to C6706. On chromosome II, 1,052 out of 1,064 annotated genes (98.9%) are shared
368 between strains, where 10 (0.94%) and 2 (0.19%) of genes are unique to N16961 and C6706,
369 respectively. Importantly, this analysis provided the genomic position for each ortholog of
370 N16961 genes present in C6706 (Dataset S1).

371

372 We used the orthologous sites to analyze each transposon mutant we sequenced (Dataset
373 S1, Fig. S2 and S3). Using the breseq annotation data, we calculated the position of the
374 transposon within each gene as a percent of basepairs into the ORF of C6706. These position
375 values were previously reported for each strain in the donor library strain N16961. To assess the
376 relationship, we performed a linear regression of our sequenced C6706 insertions with the
377 previously described N16961 from the donor library, expecting a perfect linear correlation.
378 Although 19/23 mutants had an exact match, some of our values diverged from the line of best fit
379 (Fig. 5), although there was a strong statistical correlation between the variables (Kendall’s
380 coefficient $\tau = 0.752$, $n = 23$, and $P < 0.0001$). Upon further investigation of this anomaly, we
381 discovered two categories of false negatives. In category one (Fig. S3, Panels A and B), we
382 observed two cases where genes were annotated in N16961 but not in C6706. Consequently,
383 these data points lacked a calculated value for the transposon insertion site in C6706 and thus fell

384 on the y-axis. In the second category, two false negatives were attributed to a difference in the
385 size of the gene orthologs between N16961 and C6706 (Fig. S3, Panels C and D). This
386 discrepancy resulted in a shift of the relative position reported for the transposon. After
387 accounting for these deviations and correcting the data accordingly, we confirmed that the
388 transposon inserted into the cognate position of the Grant Library mutants we sequenced with
389 100% precision.

390

391 **Co-transformation of the *luxOG319S* gain of function mutation is an infrequent event.**

392 Since we employed natural competence to transfer the transposon mutations, there is a possibility
393 that the *luxOG319S* mutation from the donor library might have been co-transformed along with
394 the transposon into the Grant library. However, unlike the strong selection pressure for the
395 transposon mutation, selection for the lux mutation would be indirect and weaker, depending on
396 whether the lux mutation provides a fitness advantage to cells allowing them to outcompete
397 wildtype cells during outgrowth in selective media.

398

399 In the 23 genome sequences analyzed above, none had the *luxOG319S* mutation.
400 However, we did consider that the frequency of transfer of *luxO* mutation could be elevated in
401 genes for which the transposon is within close genomic proximity to *luxO*. To test this, we
402 isolated gDNA from 20 randomly sampled transposon mutants in 5kb windows up to 50 kb up-
403 and downstream of *luxO* (Table S1). We then PCR amplified *luxO* and performed Sanger
404 sequencing. In only one instance did the *luxOG319S* mutation transfer into a Grant library strain
405 (Fig. 6). The absolute distance of this transposon mutant is 12,363 away from *luxO*, and three
406 mutants closer to *luxO* in this analysis did not transfer the mutation. This suggests that proximity
407 of the transposon mutations to *luxO* increases the chance of transfer of the *luxO* mutation, but its
408 transfer remains partially stochastic.

409

410 In summary, our investigation into the potential co-transfer of the *luxOG319S* mutation
411 with the transposon has shown that while it is possible, it is an infrequent event. Among the 23
412 genomes we analyzed and the additional Sanger sequencing data we collected, the *luxOG319S*
413 mutation was observed in only 1 out of 45 (0.02%) genomes, emphasizing the relative rarity of
414 this co-transfer event. However, when examining transposon insertions near *luxO* from the Grant
415 library, we recommend the sequence of *luxO* be verified.

416

417 **Natural competence in Grant library strains is IPTG inducible.** When generating the Grant
418 library, we supplemented the outgrowth media with chloramphenicol and kanamycin to select for

419 maintenance of the plasmid conferring IPTG-induced natural competence, pMMB-*tfoX-qstR*, and
420 the TnFLG3 transposon, respectively. We reasoned that a library established with strains
421 harboring this plasmid would be advantageous to the research community as it would facilitate
422 additional genome edits using chitin-independent natural competence and homologous
423 recombination upon induction with IPTG. In proof of concept for this idea, we randomly selected
424 10 mutants from the Grant library and performed a knock-in experiment of a trimethoprim (tm)
425 resistance gene. In short, we used thymol to isolate whole gDNA from a tm resistant strain and
426 added 16.2 µg of whole gDNA to our competent cells, which we prepared following our protocol
427 described in Materials and Methods.

428

429 After incubating our competent cells with gDNA overnight, we used spot plates to assess
430 antibiotic phenotypes. All the randomly selected library mutants grew on LB plates
431 supplemented with trimethoprim between dilution factors of $10^{-3} - 10^{-8}$ (Fig. 7). When also
432 plated on growth media supplemented with kanamycin, there was parity in the growth
433 phenotypes observed on tm plates for all but one mutant (strain 8C5). When we examined the
434 images of the kanamycin supplemented spot plates when the library was constructed (Fig. S1),
435 we found mutant 8C5 didn't grow there either. We posit that the spurious growth of strain 8C5
436 likely reflects a frozen subpopulation of our library recipient strain that was able to withstand
437 kanamycin during outgrowth or contamination introduced during the spot-plate assay. Taken
438 together, all the library mutants we tested could undergo additional genome edits with overnight
439 induction of natural competence.

440

441 **Differential motility responses of recipient library mutants reveal unappreciated epistasis**
442 **exists in donor library.** *V. cholerae* exhibits high motility by virtue of a single polar flagellum,
443 a characteristic that contributes significantly to its pathogenesis. *V. cholerae* isolated from active
444 infections display increased motility compared to lab-grown strains (56) and demonstrated a
445 heightened ability to colonize hosts (57). Moreover, motility allows *V. cholerae* to survive in its
446 aquatic environment, enabling it to swim freely as planktonic cells or form biofilms in response
447 to environmental stress. Furthermore, previous work has demonstrated the involvement of least
448 40 genes in flagellum biosynthesis and motility, classified into temporally distinct classes (I
449 through IV) (58–60). Notably, some of these genes are known to trigger an immune response
450 (56).

451

452 Motility is an easily screened phenotype, and the functional consequences of null
453 flagellar gene mutants are well established. Therefore, Cameron et al., 2008 (32), employed

454 motility assays as one of the validation metrics for their constructed library. In this context, we
455 also measured motility of the Grant library null flagellar gene mutants. By performing the assay
456 using paired mutants from the donor and recipient libraries, we reasoned that we would foremost
457 independently confirm the motility phenotypes reported by Cameron et. al., 2008. Furthermore,
458 previous studies have indicated that genes in classes III and IV of the flagellum biosynthesis
459 hierarchy exhibit cell-density dependent phenotypes (61). Thus, the motility assay would serve to
460 provide supporting evidence for or against our hypothesis that quorum sensing epistasis is a
461 missing feature of the donor library.

462

463 Out of the 33 genes we examined, we successfully replicated the motility phenotype
464 reported for the donor library's nonmotile mutants in all but one strain (*fliR*) (Fig. 8).
465 Additionally, we observed that both libraries exhibited nonmotile behavior for *rpoN* (class I) and
466 *flaA*, (class III) that are essential for expression of the flagellar biosynthesis genes (Fig. 8).
467 Furthermore, motility was also abolished for the σ -54 dependent transcriptional regulator
468 transposon mutants of *fliA* (class I) in both libraries, consistent with previous observations (62).
469 When comparing motility within classes, paired null mutants from the Cameron and Grant
470 libraries displayed similar movement on the plates for all classes, except for class III, where a
471 statistically significant difference was observed (Table 1, two-tailed *t*-test: $P = 0.012$).
472 Additionally, two mutant pairs (*flgM* and *flgN*) within class IV biosynthesis genes exhibited
473 opposite motility phenotypes. While these opposing effects were observed within the same class,
474 the net effect of class IV genes canceled each other out in the statistical analysis, so this class
475 comparison was insignificant. Taken together, our results suggest quorum sensing epistasis with
476 motility genes results in the different motility outcomes as the donor library is locked in a low-
477 cell density genomic background. Our finding is supported by several other research groups who
478 as well have observed nuances in different phenotypes resulting from differences in genomic
479 background (48)

480

481 Conclusion

482 Bacteria employ quorum sensing (QS) to regulate gene expression based on population density.
483 In the case of *V. cholerae*, the etiological agent of cholera, QS controls various phenotypes as the
484 population transitions between low and high cell density. Researchers previously constructed an
485 ordered mutant library, systematically disrupting every non-essential gene in *V. cholerae* with a
486 transposon insertion. However, unbeknownst to them, this library was created in a strain with a
487 mutation that rendered the mutants incapable of transitioning between low and high cell density.
488

489 In this study, we successfully transferred transposon insertions from these *V. cholerae*
490 non-redundant ordered mutants into a wildtype genetic background using chitin-independent
491 natural transformation. The resulting Grant Library comprises 3,102 mutants, covering
492 approximately 79.8% of the ORFs annotated in *V. cholerae*.
493

494 In addition to encoding a functional quorum sensing system, another notable advantage
495 of the Grant Library is that we selected for the transposon insertion and the plasmid that confers
496 IPTG-inducible natural competence during outgrowth in selective media. Accordingly, upon
497 induction with IPTG, mutants from the Grant Library can undergo additional genome edits when
498 co-incubated with gDNA. Furthermore, growth in the absence of selection leads to rapid curing
499 of the competence plasmid if it is not needed. These features make the Grant Library an
500 invaluable resource for studying pleiotropic and epistatic genetic interactions in *V. cholerae*,
501 including combinations that are synthetically lethal. Such information will be invaluable toward
502 generating new therapeutic options to treat *V. cholerae* infections.
503

504 Construction of the Grant Library was aided by a novel, in-house gDNA extraction
505 method we developed based on thymol cell lysis. Our use of thymol allowed extraction of gDNA
506 in a highly efficient and economical way, producing DNA that was usable in several downstream
507 applications. Indeed, as many as 576 manual gDNA extractions were performed in a single
508 workday. We have tested the efficiency of thymol treatment on several other biological
509 specimens including bacteria in gram -negative and -positive staining classes and yeast. Among
510 our test strains, gDNA yield was highest for *V. cholerae* (~ 22 ng/μl), although most strains
511 yielded some gDNA (2 – 8 ng/μl) (data not shown). The apparent vibrio-specificity of thymol
512 treatment is an interesting avenue for further research as its understanding can provide additional
513 insight into its antibacterial activity, potentially contributing to novel disease control strategies.
514 In summary, the Grant Library complements the non-redundant library made in the quorum-
515 incompetent strain, and the methods used to construct it, a valuable approach toward
516 understanding *V. cholerae* evolutionary genetics.
517

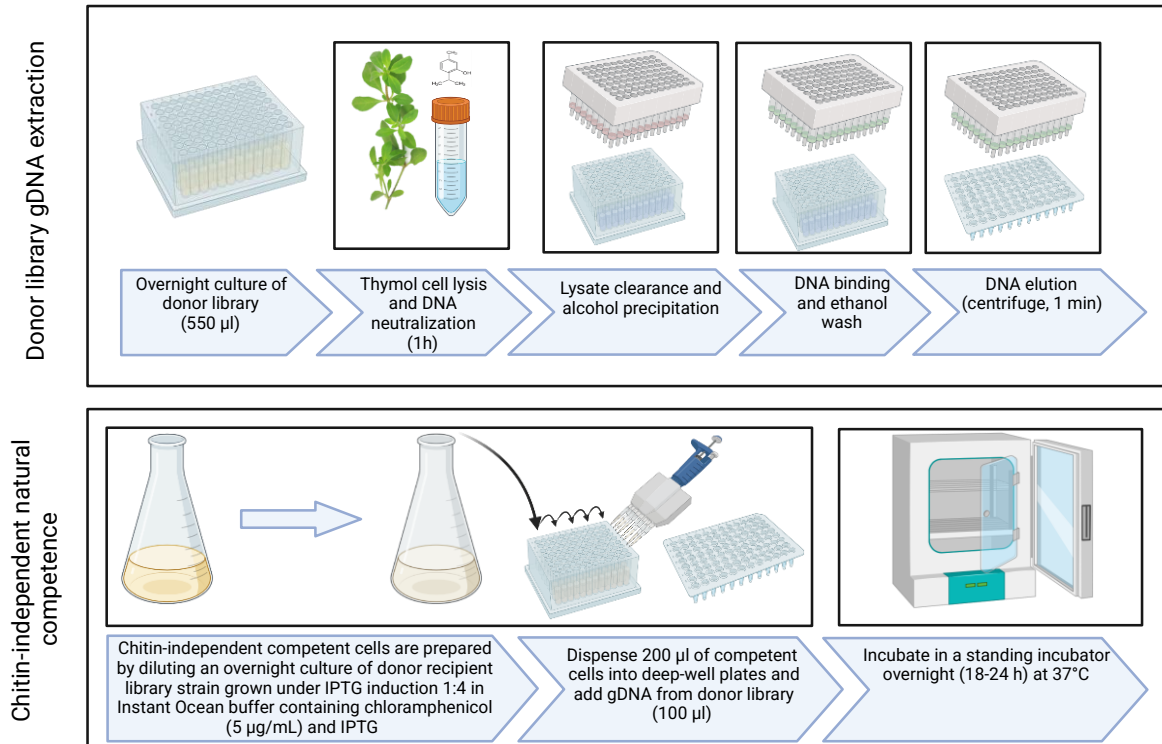
518 Acknowledgements

519 We thank Ewen Cameron and the John Mekalanos lab for constructing the 2008 *V. cholerae* non-
520 redundant library, Vic DiRita for granting access to a copy of the collection, and Bonnie Bassler
521 and Julie Valastyan for providing plates that were missing from the DiRita collection. We also
522 thank Ankur Dalia for providing the plasmid conferring natural competence. This work was
523 supported by National Institutes of Health Grants GM139537 and AI158433 to C.M.W and a

524 NIGMS Diversity Supplement to N.A.G. Financial support was also received from The
525 BEACON Center for the Study of Evolution in Action at Michigan State University (to N.A.G.).
526

527 **Figures and Tables**

528



529
530 Figure 1. Thymol-Assisted gDNA extraction and chitin-independent natural transformation.
531 Overnight cultures of the donor library were grown in 550 μ l of selective media (LB +
532 kanamycin). After overnight growth, the samples were centrifuged, the supernatant was
533 aspirated, and the cell pellets were incubated for one hour at 64°C in a novel gDNA extraction
534 buffer containing thymol. gDNA was then isolated from the clarified supernatant using an
535 alcohol precipitation method, followed by resuspension of the gDNA in 1x TE buffer. In parallel,
536 a quorum-competent wildtype *V. cholerae* strain carrying the plasmid conferring natural
537 competence (pMMB-*tfoX-qstR*) was grown in selective media (LB + chloramphenicol)
538 supplemented with IPTG. The next day, competent cells were diluted 1:4 in 0.5x Instant Ocean,
539 to which chloramphenicol and IPTG were added. Subsequently, 200 μ l of cells were dispensed
540 into the wells of a deep-well 96-well plate and co-incubated with 100 μ l of our gDNA extraction

541 buffer at 30°C for 18 – 24 h. For a detailed description, refer to the Materials and Methods
542 section.

543

544

545

		Has transposon	Does not have transposon	Measure	Value	
Identified as having the transposon	3102	15	22	71	Sensitivity	0.9930
					Specificity	0.8256
Identified as not having the transposon					Precision	0.9952
					Negative Predictive Value	0.7634
				False Positive Rate	0.1744	
				False Discovery Rate	0.0048	
				False Negative Rate	0.0070	
				Accuracy	0.9885	
				F1 Score	0.9941	
				Matthews Correlation Coefficient	0.7880	

546

547

548 Figure 2. Analysis of Library Transfer. The outcomes of growth on selective media for each
549 mutant were recorded after chitin-independent natural transformation of the donor library. These
550 values were utilized as inputs to construct a 2x2 confusion matrix, categorizing the results as
551 follows: True Positives (3,102 wells), False Negatives (22 wells), True Negatives (71 wells), and
552 False Positives (15 wells). The accompanying table presents the calculated measures, the values
553 of which were computed using standard derivations.

554

Unassigned new junction evidence										
	seq id	position	reads (cov)	reads (cov)	score	skew	freq	annotation	gene	product
	?_NZ_CP046845	151866 =	2 (0.050)					coding (225/543 nt)	GPY04_RS15290	N-acetyltransferase
*	?_pSC189	= 4058	0 (0.000)	37 (0.780)	15/290	0.0	97.4%	intergenic (+121/+620)	aph(3')-II (or nptII)/traJ	aminoglycoside phosphotransferase from Tn5/oriT-recognizing protein
	?_NZ_CP046845	= 151868	2 (0.050)					coding (227/543 nt)	GPY04_RS15290	N-acetyltransferase
*	?_pSC189	1802 =	0 (0.000)	25 (0.520)	14/292	0.0	96.2%	intergenic (-/-41)	-/3xFLAG	~/three tandem FLAG(R) epitope tags, followed by an enterokinase cleavage site

555

556

557 Figure 3. Representative sample of breseq output showing new junction evidence supporting
558 transposon insertion. The figure shows a portion of the summary.html file generated for a breseq
559 analysis run. In this example, a new junction has been called between chromosome II
560 (NZ_CP046845) of *V. cholerae* strain C6706 and the plasmid (pSC189) containing
561 representative sequences of the transposon. Insertions have left and right boundaries, where the
562 chromosome and sequence meet. The boundaries are marked with an asterisk. The annotation
563 column shows the position of the transposon within the gene (GPY04_RS15290), which we
564 converted to a value called “percent into open reading frame.” In this example, that value is
565 41.43% ((225/543) * 100)). This value was calculated for all strains sequenced in this study.

566

567

568

569

570

571

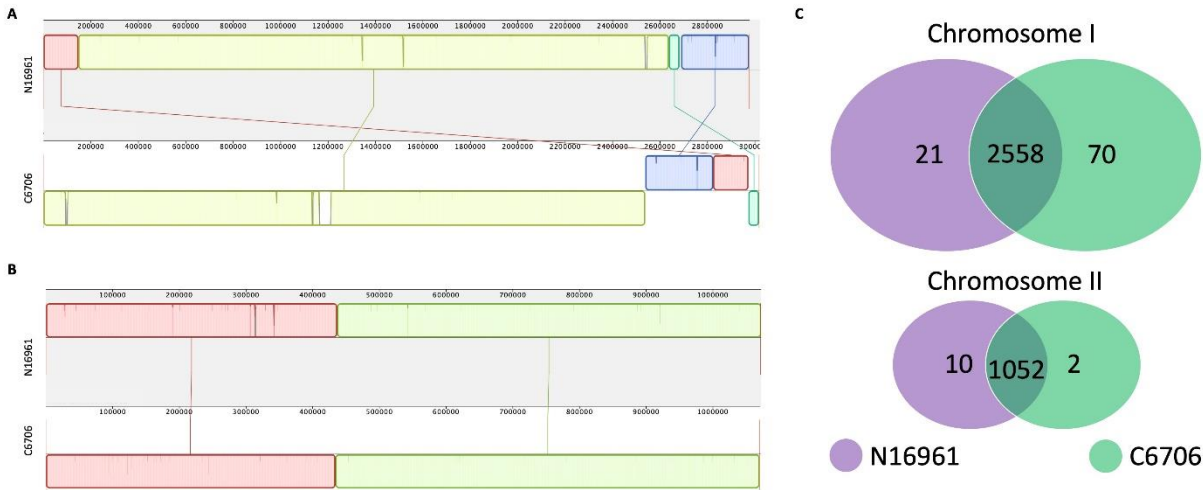
572

573

574

575

576

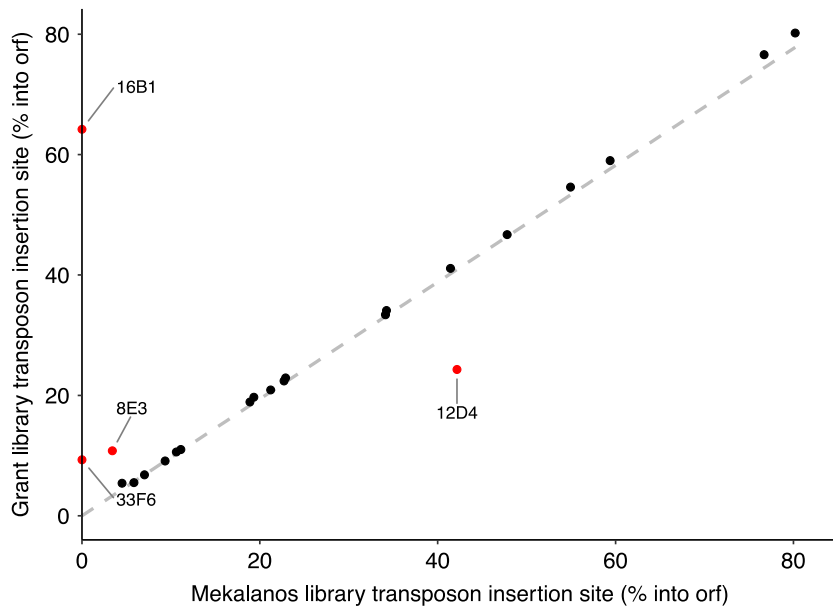


577

578

579 Figure 4. Genomic comparative analysis of *V. cholerae* N16961 and C6706 for chromosome I
580 (A) and chromosome II (B). Genbank files for whole-genome sequences of chromosomes I and
581 II of both strains were downloaded from NCBI. The analysis involved a comparative
582 examination of genetic variations and conservation patterns between the two strains. *V. cholerae*
583 strain N16961 is shown with a gray background and C6706 a white one. Genome segments are
584 shown as colored colinear blocks centered around the “positive” and “negative” strands of each
585 chromosome. Lines connecting the segments show their orthologous alignments between the
586 strains, including inversions. Panel C is a Venn diagram summarizing the relationship of genes
587 for each strain and chromosome. The data underlying the illustration in panel C, including the
588 genomic position of orthologous gene pairs, is provided in the Supplementary Information
589 (Datasets S2–S4).

590

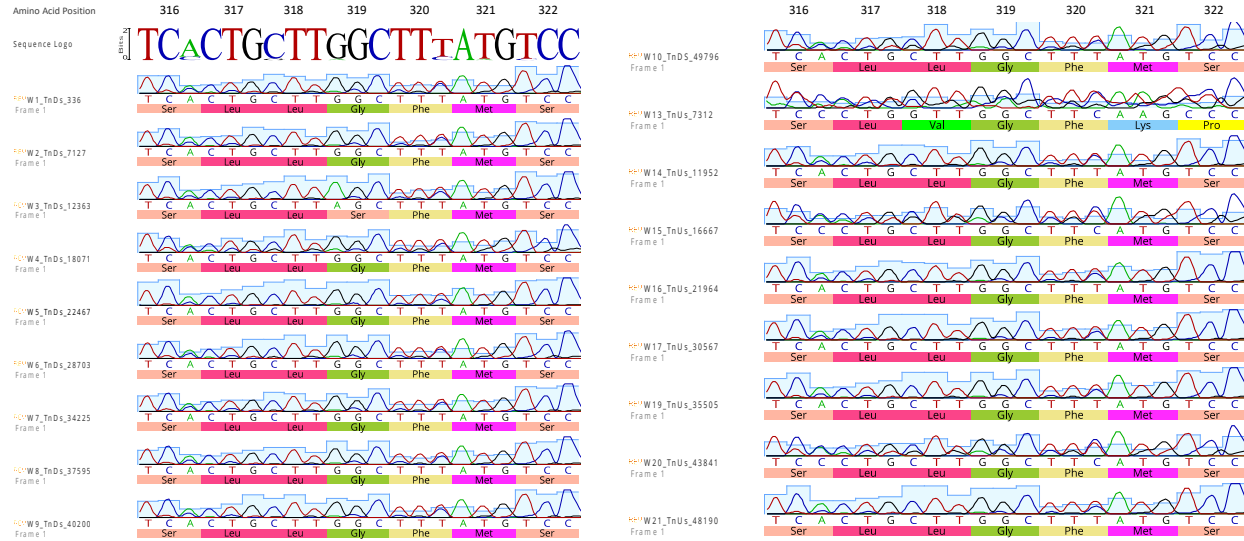


591

592 Figure 5. Correlation between transposon insertion sites in *V. cholerae* N16961 and C6706. Each
593 point represents the transposon insertion site, calculated as percent into open reading frame. The
594 values for strain N16961 were reported in supplementary dataset 3 of Cameron et al. (2008), and
595 in this work, they were calculated using the data provided in the annotation column of the breseq
596 output (Fig. 3). The correlation analysis yields a strong positive correlation with Kendall's
597 coefficient $\tau = 0.752$ ($n = 23$, and $P << 0.0001$), indicating a significant relationship between the
598 insertion sites of the two strains.

599

600

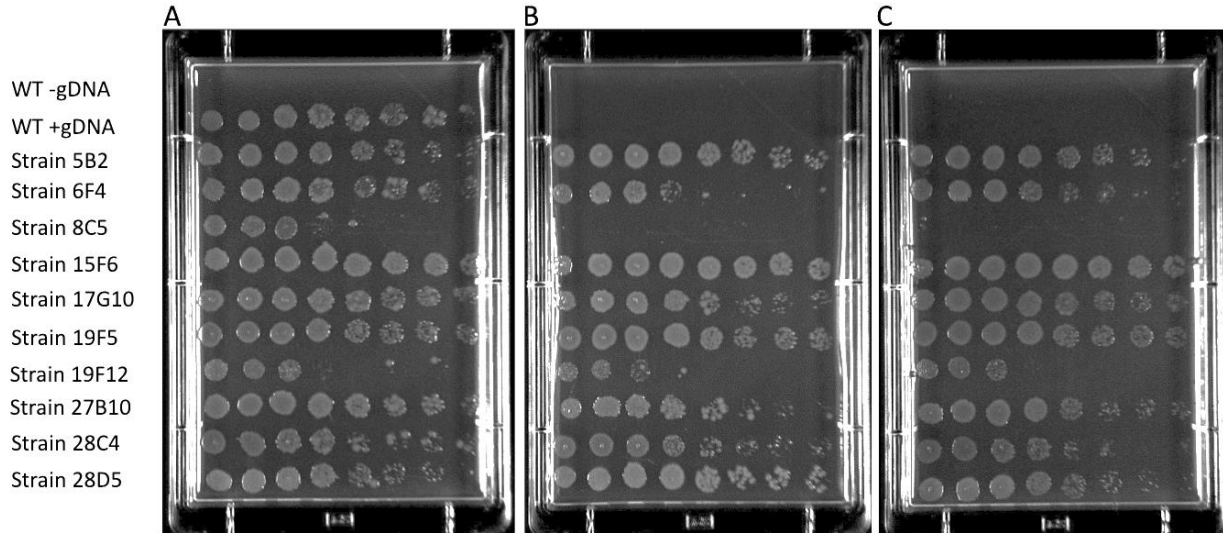


601

602

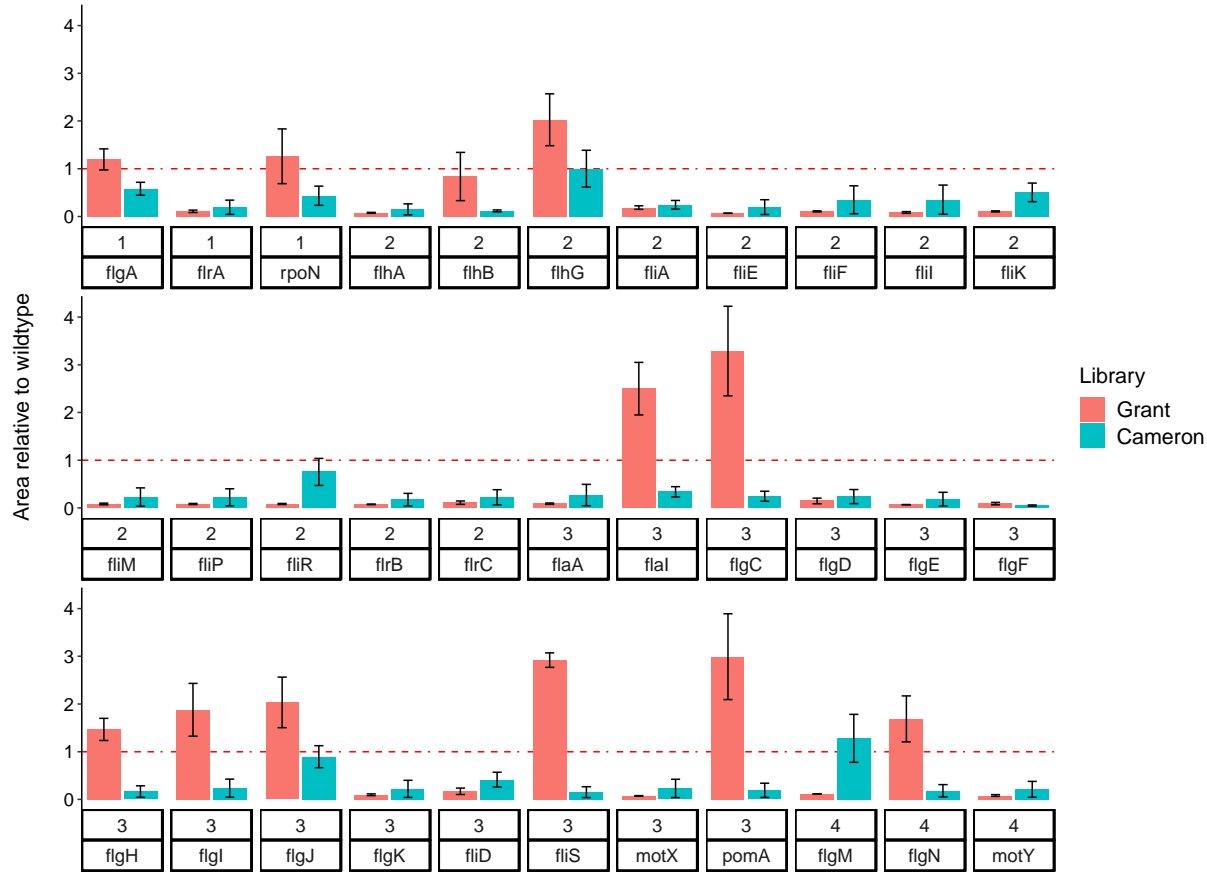
603 Figure 6. Sanger sequence genome alignments. We randomly selected Grant library transposon
604 mutants in 5kb windows up to 50 kp up- and downstream of *luxO*. Subsequently, we isolated
605 gDNA and processed samples for Sanger sequencing. Each row shows a randomly selected
606 transposon mutant (Tn) and their absolute distance downstream (Ds) or upstream (Us) of *luxO*.
607 The gain of function mutation in *luxO* is annotated as a glycine to serine mutation at amino acid
608 position 319. Our Sanger sequencing analysis identified this mutation in one mutant
609 (W3_TnDs_12363), indicating the mutation transfers at low frequency and only in genes within
610 close proximity to *luxO*.

611



612

613 Figure 7. Chromosomal integration of a trimethoprim resistant gene in select mutants from the
614 Grant library using IPTG-induced natural competence. We induced natural competence in
615 wildtype *V. cholerae* strain C6706 carrying plasmid pMMB-*tfoX-qstR* (NG001) and 10 randomly
616 selected mutants from the Grant library according to procedure described in Materials and
617 Methods. These strains were then co-incubated with gDNA extracted from a strain carrying a
618 trimethoprim resistant cassette and on the following day spotted on antibiotic selection media.
619 All the strains carrying the plasmid grew on plates supplemented with trimethoprim (Panel A).
620 On the plate with kanamycin (Panel B) or kanamycin + trimethoprim (Panel C), all strains grew
621 except strain 8C5, indicating that this strain does not have a transposon insertion.



638 Table 1. Two-sided *t*-test results comparing the motility of paired Grant and Cameron et. al.,
639 (2008). Flagellar mutants assayed in this study are grouped by the flagellar biosynthesis gene
640 cluster (I-IV) they belong to.

641

Cluster	Sample size (n)	Mean difference	df	<i>t</i>	<i>P</i>
I	3	0.452	2	1.64	0.242
II	13	-0.045	12	-0.37	0.720
III	14	0.999	13	2.92	0.012
IV	3	0.072	2	0.09	0.935

642

643

644

645 **References**

- 646 1. M. Ali, A. R. Nelson, A. L. Lopez, D. A. Sack, Updated Global Burden of Cholera in
647 Endemic Countries. *PLOS Neglected Tropical Diseases* **9**, e0003832 (2015).
- 648 2. I. Ilic, M. Ilic, Global Patterns of Trends in Cholera Mortality. *Trop Med Infect Dis* **8**, 169
649 (2023).
- 650 3. D. Legros, Global Cholera Epidemiology: Opportunities to Reduce the Burden of Cholera
651 by 2030. *J Infect Dis* **218**, S137–S140 (2018).
- 652 4. , Roadmap 2030 – Global Task Force on Cholera Control (October 22, 2023).
- 653 5. D. Lippi, E. Gotuzzo, S. Caini, Cholera. *Microbiology Spectrum* **4**,
654 10.1128/microbiolspec.poh-0012-2015 (2016).
- 655 6. S. Yamai, T. Okitsu, T. Shimada, Y. Katsume, Distribution of serogroups of *Vibrio cholerae*
656 non-O1 non-O139 with specific reference to their ability to produce cholera toxin, and
657 addition of novel serogroups. *Kansenshogaku Zasshi* **71**, 1037–1045 (1997).
- 658 7. A. Safa, G. B. Nair, R. Y. C. Kong, Evolution of new variants of *Vibrio cholerae* O1.
659 *Trends in Microbiology* **18**, 46–54 (2010).
- 660 8. J. B. Kaper, J. G. Morris, M. M. Levine, Cholera. *Clin Microbiol Rev* **8**, 48–86 (1995).

661 9. D. Hu, *et al.*, Origins of the current seventh cholera pandemic. *Proceedings of the National*
662 *Academy of Sciences* **113**, E7730–E7739 (2016).

663 10. K. Okada, T. Iida, K. Kita-Tsukamoto, T. Honda, Vibrios Commonly Possess Two
664 Chromosomes. *J Bacteriol* **187**, 752–757 (2005).

665 11. S. Sozhamannan, T. Waldminghaus, Exception to the exception rule: synthetic and
666 naturally occurring single chromosome *Vibrio cholerae*. *Environmental Microbiology* **22**,
667 4123–4132 (2020).

668 12. D. K. Karaolis, R. Lan, P. R. Reeves, The sixth and seventh cholera pandemics are due to
669 independent clones separately derived from environmental, nontoxigenic, non-O1 *Vibrio*
670 *cholerae*. *J Bacteriol* **177**, 3191–3198 (1995).

671 13. S. M. Faruque, *et al.*, Emergence and evolution of *Vibrio cholerae* O139. *Proceedings of*
672 *the National Academy of Sciences* **100**, 1304–1309 (2003).

673 14. T. Ramamurthy, *et al.*, Revisiting the Global Epidemiology of Cholera in Conjunction With
674 the Genomics of *Vibrio cholerae*. *Front Public Health* **7**, 203 (2019).

675 15. S. N. Sakib, G. Reddi, S. Almagro-Moreno, Environmental Role of Pathogenic Traits in
676 *Vibrio cholerae*. *J Bacteriol* **200**, e00795-17 (2018).

677 16. Y. Sun, E. E. Bernardy, B. K. Hammer, T. Miyashiro, Competence and Natural
678 Transformation in Vibrios. *Mol Microbiol* **89**, 10.1111/mmi.12307 (2013).

679 17. R. L. Marvig, M. Blokesch, Natural transformation of *Vibrio cholerae* as a tool -
680 Optimizing the procedure. *BMC Microbiology* **10**, 155 (2010).

681 18. S. Stutzmann, M. Blokesch, Comparison of chitin-induced natural transformation in
682 pandemic *Vibrio cholerae* O1 El Tor strains. *Environ Microbiol* **22**, 4149–4166 (2020).

683 19. K. L. Meibom, M. Blokesch, N. A. Dolganov, C.-Y. Wu, G. K. Schoolnik, Chitin Induces
684 Natural Competence in *Vibrio cholerae*. *Science* **310**, 1824–1827 (2005).

685 20. S. S. Watve, J. Thomas, B. K. Hammer, CytR Is a Global Positive Regulator of
686 Competence, Type VI Secretion, and Chitinases in *Vibrio cholerae*. *PLoS One* **10**,
687 e0138834 (2015).

688 21. M. Lo Scrudato, S. Borgeaud, M. Blokesch, Regulatory elements involved in the expression
689 of competence genes in naturally transformable *Vibrio cholerae*. *BMC Microbiology* **14**,
690 327 (2014).

691 22. M. L. Scrudato, M. Blokesch, The Regulatory Network of Natural Competence and
692 Transformation of *Vibrio cholerae*. *PLOS Genetics* **8**, e1002778 (2012).

693 23. E. S. Antonova, B. K. Hammer, Genetics of Natural Competence in *Vibrio cholerae* and
694 other Vibrios. *Microbiol Spectr* **3**, 3.3.20 (2015).

695 24. A. B. Dalia, D. W. Lazinski, A. Camilli, Identification of a Membrane-Bound
696 Transcriptional Regulator That Links Chitin and Natural Competence in *Vibrio cholerae*.
697 *mBio* **5**, 10.1128/mbio.01028-13 (2014).

698 25. T. N. Dalia, *et al.*, Multiplex genome editing by natural transformation (MuGENT) for
699 synthetic biology in *Vibrio natriegens*. *ACS Synth Biol* **6**, 1650–1655 (2017).

700 26. A. B. Dalia, “Natural Cotransformation and Multiplex Genome Editing by Natural
701 Transformation (MuGENT) of *Vibrio cholerae*” in *Vibrio Cholerae: Methods and*
702 *Protocols*, Methods in Molecular Biology., A. E. Sikora, Ed. (Springer, 2018), pp. 53–64.

703 27. A. B. Dalia, E. McDonough, A. Camilli, Multiplex genome editing by natural
704 transformation. *Proc Natl Acad Sci U S A* **111**, 8937–8942 (2014).

705 28. T. Baba, *et al.*, Construction of *Escherichia coli* K-12 in-frame, single-gene knockout
706 mutants: the Keio collection. *Mol Syst Biol* **2**, 2006.0008 (2006).

707 29. M. M. Pearson, S. Pahil, V. S. Forsyth, A. E. Shea, H. L. T. Mobley, Construction of an
708 Ordered Transposon Library for Uropathogenic *Proteus mirabilis* HI4320. *Microbiol Spectr*
709 **10**, e03142-22.

710 30. B. Ramage, *et al.*, Comprehensive Arrayed Transposon Mutant Library of *Klebsiella*
711 *pneumoniae* Outbreak Strain KPNIH1. *Journal of Bacteriology* **199**, 10.1128/jb.00352-17
712 (2017).

713 31. P. D. Fey, *et al.*, A Genetic Resource for Rapid and Comprehensive Phenotype Screening of
714 Nonessential *Staphylococcus aureus* Genes. *mBio* **4**, 10.1128/mbio.00537-12 (2013).

715 32. D. E. Cameron, J. M. Urbach, J. J. Mekalanos, A defined transposon mutant library and its
716 use in identifying motility genes in *Vibrio cholerae*. *Proceedings of the National Academy of
717 Sciences* **105**, 8736–8741 (2008).

718 33. H. Rui, *et al.*, Reactogenicity of live-attenuated *Vibrio cholerae* vaccines is dependent on
719 flagellins. *Proceedings of the National Academy of Sciences* **107**, 4359–4364 (2010).

720 34. R. W. Bogard, B. W. Davies, J. J. Mekalanos, MetR-Regulated *Vibrio cholerae* Metabolism
721 Is Required for Virulence. *mBio* **3**, 10.1128/mbio.00236-12 (2012).

722 35. T. G. Dong, B. T. Ho, D. R. Yoder-Himes, J. J. Mekalanos, Identification of T6SS-
723 dependent effector and immunity proteins by Tn-seq in *Vibrio cholerae*. *Proceedings of the
724 National Academy of Sciences* **110**, 2623–2628 (2013).

725 36. A. J. Van Alst, V. J. DiRita, Aerobic Metabolism in *Vibrio cholerae* Is Required for
726 Population Expansion during Infection. *mBio* **11**, 10.1128/mbio.01989-20 (2020).

727 37. S. T. Miyata, D. Unterweger, S. P. Rudko, S. Pukatzki, Dual Expression Profile of Type VI
728 Secretion System Immunity Genes Protects Pandemic *Vibrio cholerae*. *PLOS Pathogens* **9**,
729 e1003752 (2013).

730 38. A. Hsiao, Z. Liu, A. Joelsson, J. Zhu, *Vibrio cholerae* virulence regulator-coordinated
731 evasion of host immunity. *Proceedings of the National Academy of Sciences* **103**, 14542–
732 14547 (2006).

733 39. F. P. Rothenbacher, J. Zhu, Efficient responses to host and bacterial signals during *Vibrio*
734 *cholerae* colonization. *Gut Microbes* **5**, 120–128 (2014).

735 40. S. Saha, S. Aggarwal, D. V. Singh, Attenuation of quorum sensing system and virulence in
736 *Vibrio cholerae* by phytomolecules. *Frontiers in Microbiology* **14** (2023).

737 41. J. Zhu, *et al.*, Quorum-sensing regulators control virulence gene expression in *Vibrio*
738 *cholerae*. *Proceedings of the National Academy of Sciences* **99**, 3129–3134 (2002).

739 42. J. Zhu, J. J. Mekalanos, Quorum Sensing-Dependent Biofilms Enhance Colonization in
740 *Vibrio cholerae*. *Developmental Cell* **5**, 647–656 (2003).

741 43. M. Jemielita, N. S. Wingreen, B. L. Bassler, Quorum sensing controls *Vibrio cholerae*
742 multicellular aggregate formation. *eLife* **7**, e42057 (2018).

743 44. M. M. Hoque, *et al.*, Quorum Regulated Resistance of *Vibrio cholerae* against
744 Environmental Bacteriophages. *Sci Rep* **6**, 37956 (2016).

745 45. H. Boyaci, *et al.*, Structure, Regulation, and Inhibition of the Quorum-Sensing Signal
746 Integrator LuxO. *PLoS Biol* **14**, e1002464 (2016).

747 46. R. Herzog, N. Peschek, K. S. Fröhlich, K. Schumacher, K. Papenfort, Three autoinducer
748 molecules act in concert to control virulence gene expression in *Vibrio cholerae*. *Nucleic
749 Acids Res* **47**, 3171–3183 (2019).

750 47. S. A. Jung, C. A. Chapman, W.-L. Ng, Quadruple Quorum-Sensing Inputs Control *Vibrio
751 cholerae* Virulence and Maintain System Robustness. *PLOS Pathogens* **11**, e1004837
752 (2015).

753 48. S. Stutzmann, M. Blokesch, Circulation of a Quorum-Sensing-Impaired Variant of *Vibrio
754 cholerae* Strain C6706 Masks Important Phenotypes. *mSphere* **1**, 10.1128/msphere.00098-
755 16 (2016).

756 49. A. Escobar, M. Pérez, G. Romanelli, G. Blustein, Thymol bioactivity: A review focusing on
757 practical applications. *Arabian Journal of Chemistry* **13**, 9243–9269 (2020).

758 50. J. B. Brown, Classifiers and their Metrics Quantified. *Mol Inform* **37**, 1700127 (2018).

759 51. D. E. Deatherage, J. E. Barrick, Identification of mutations in laboratory evolved microbes
760 from next-generation sequencing data using breseq. *Methods Mol Biol* **1151**, 165–188
761 (2014).

762 52. A. C. E. Darling, B. Mau, F. R. Blattner, N. T. Perna, Mauve: Multiple Alignment of
763 Conserved Genomic Sequence With Rearrangements. *Genome Res* **14**, 1394–1403 (2004).

764 53. M. Kearse, *et al.*, Geneious Basic: An integrated and extendable desktop software platform
765 for the organization and analysis of sequence data. *Bioinformatics* **28**, 1647–1649 (2012).

766 54. J. Schindelin, *et al.*, Fiji: an open-source platform for biological-image analysis. *Nat
767 Methods* **9**, 676–682 (2012).

768 55. J. F. Heidelberg, *et al.*, DNA sequence of both chromosomes of the cholera pathogen *Vibrio
769 cholerae*. *Nature* **406**, 477–483 (2000).

770 56. M. Grognot, A. Mittal, M. Mah'moud, K. M. Taute, *Vibrio cholerae* Motility in Aquatic
771 and Mucus-Mimicking Environments. *Applied and Environmental Microbiology* **87**,
772 e01293-21 (2021).

773 57. F. Khan, N. Tabassum, R. Anand, Y.-M. Kim, Motility of *Vibrio* spp.: regulation and
774 controlling strategies. *Appl Microbiol Biotechnol* **104**, 8187–8208 (2020).

775 58. M. A. Echazarreta, K. E. Klose, *Vibrio* Flagellar Synthesis. *Frontiers in Cellular and*
776 *Infection Microbiology* **9** (2019).

777 59. K. A. Syed, *et al.*, The *Vibrio cholerae* Flagellar Regulatory Hierarchy Controls Expression
778 of Virulence Factors. *J Bacteriol* **191**, 6555–6570 (2009).

779 60. S. Zhu, S. Kojima, M. Homma, Structure, gene regulation and environmental response of
780 flagella in *Vibrio*. *Frontiers in Microbiology* **4** (2013).

781 61. S. Beyhan, A. D. Tischler, A. Camilli, F. H. Yildiz, Transcriptome and Phenotypic
782 Responses of *Vibrio cholerae* to Increased Cyclic di-GMP Level. *J Bacteriol* **188**, 3600–
783 3613 (2006).

784 62. D. S. Millikan, E. G. Ruby, FlrA, a σ54-Dependent Transcriptional Activator in *Vibrio*
785 *fischeri*, Is Required for Motility and Symbiotic Light-Organ Colonization. *J Bacteriol* **185**,
786 3547–3557 (2003).

787